New Phytologist

Research

Contrasting cadmium resistance strategies in two metallicolous populations of *Arabidopsis halleri*

Massimiliano Corso[1], M. Sol Schvartzman[2], Flavia Guzzo[3], Florence Souard[4,5], Eugeniusz Malkowski[6], Marc Hanikenne[2] and Nathalie Verbruggen[1]

[1]Laboratory of Plant Physiology and Molecular Genetics, Université Libre de Bruxelles, 1050 Brussels, Belgium; [2]InBioS-PhytoSystems, Functional Genomics and Plant Molecular Imaging, University of Liège, B-4000 Liège, Belgium; [3]Department of Biotechnology, University of Verona, 37134 Verona, Italy; [4]Département de Pharmacochimie Moléculaire, CNRS UMR5063, University Grenoble Alpes, 38400, St Martin d'Hères, France; [5]Laboratoire de Pharmacognosie, de Bromatologie et de Nutrition Humaine, Université Libre de Bruxelles, 1050 Brussels, Belgium; [6]Department of Plant Physiology, Faculty of Biology and Environmental Protection, University of Silesia in Katowice, 40-032 Katowice, Poland

Author for correspondence:
Nathalie Verbruggen
Tel: +32 2 6502128
Email: nverbru@ulb.ac.be

Received: *8 September 2017*
Accepted: *5 November 2017*

New Phytologist (2017)
doi: 10.1111/nph.14948

Key words: Arabidopsis, cadmium exclusion, cadmium hyperaccumulation, ionomic, metabolomic, phenylpropanoids, RNA sequencing, transporter.

Summary

- While cadmium (Cd) tolerance is a constitutive trait in the *Arabidopsis halleri* species, Cd accumulation is highly variable. Recent adaptation to anthropogenic metal stress has occurred independently within the genetic units of *A. halleri* and the evolution of different mechanisms involved in Cd tolerance and accumulation has been suggested.
- To gain a better understanding of the mechanisms underlying Cd tolerance and accumulation in *A. halleri*, ionomic inductively coupled plasma mass spectrometry (ICP-MS), transcriptomic (RNA sequencing) and metabolomic (high-performance liquid chromatography–mass spectrometry) profiles were analysed in two *A. halleri* metallicolous populations from different genetic units (PL22 from Poland and I16 from Italy).
- The PL22 and I16 populations were both hypertolerant to Cd, but PL22 hyperaccumulated Cd while I16 behaved as an excluder both *in situ* and when grown hydroponically. The observed hyperaccumulator vs excluder behaviours were paralleled by large differences in the expression profiles of transporter genes. Flavonoid-related transcripts and metabolites were strikingly more abundant in PL22 than in I16 shoots. The role of novel *A. halleri* candidate genes possibly involved in Cd hyperaccumulation or exclusion was supported by the study of corresponding *A. thaliana* knockout mutants.
- Taken together, our results are suggestive of the evolution of divergent strategies for Cd uptake, transport and detoxification in different genetic units of *A. halleri*.

Introduction

Metal-hyperaccumulating plants have attracted the interest of the scientific community for over a century. Among these rare species, *Arabidopsis halleri* is a facultative hyperaccumulator used as a model to study metal homeostasis and the evolution of adaptation to extreme environments (Verbruggen *et al.*, 2009, 2013; Krämer, 2010; Hanikenne & Nouet, 2011). The *A. halleri* species shows higher cadmium (Cd) tolerance than the related *Arabidopsis thaliana* and *Arabidopsis lyrata* species (Meyer *et al.*, 2015).

High variability of Cd tolerance and accumulation exists within populations of *A. halleri*. On average, the nonmetallicolous populations are less tolerant than the metallicolous populations (Meyer *et al.*, 2015). Some *A. halleri* populations are able to accumulate extremely high Cd, as well as zinc (Zn) and lead (Pb), concentrations in their shoots (Meyer *et al.*, 2015; Stein *et al.*, 2016) through the constitutive high expression and duplication of key genes involved in metal uptake, transport/translocation and detoxification (Becher *et al.*, 2004; Weber *et al.*, 2004, 2006; Talke *et al.*, 2006; Hanikenne *et al.*, 2008; Clemens, 2017). In plants, little information is available on genes responsible for Cd uptake from the soil. Indeed, only the iron (Fe(II)) transporter IRON-REGULATED TRANSPORTER 1 (IRT1) was demonstrated to transport Cd into *A. thaliana* roots (Vert *et al.*, 2002). *HEAVY METAL ATPAse 4* (*HMA4*), which is triplicated in the *A. halleri* genome, plays a pivotal role in root-to-shoot Cd and Zn translocation and metal distribution in the shoot (Hanikenne *et al.*, 2008). Regarding detoxification mechanisms, plants have evolved different strategies to cope with the Cd-induced production of reactive oxygen species (ROS) which can cause cellular damage (Jozefczak *et al.*, 2015). One strategy is efficient Cd chelation followed by vacuolar sequestration (e.g. via phytochelatin binding) or by direct transport into the vacuole, which can be mediated by HMA3 and Cation Exchanger (CAX) 2 and 4 (Bashir *et al.*, 2016). Another strategy proposed for both *A. thaliana* and *A. halleri* is the activation of antioxidant mechanisms or the prevention of ROS accumulation by

CAX1-mediated cytosolic calcium (Ca) sequestration in vacuoles to avoid the Ca–ROS positive feedback loop (Baliardini *et al.*, 2015, 2016).

In order to gain a better understanding of the mechanisms underlying Cd tolerance and accumulation in *A. halleri*, it is crucial to take into account the evolutionary history of this species. *Arabidopsis halleri* is a self-incompatible and outcrossing Brassicaceae species with a large distribution in Europe and Far East Asia (Novikova *et al.*, 2016). According to phylogeographic studies, the populations on nonmetallicolous sites are believed to represent native populations that later independently founded the nearby populations on metallicolous sites during industrial times (Pauwels *et al.*, 2012). High variability for metal tolerance and accumulation exists among *A. halleri* populations of different geographical origins (Meyer *et al.*, 2015; Stein *et al.*, 2016). Populations collected on metallicolous sites displayed enhanced Cd tolerance compared with populations collected on nonmetallicolous sites. These results suggest that metal hypertolerance could have evolved secondarily in metallicolous environments and could involve different genes according to the population origin or genetic unit (GU). To date, the molecular mechanisms underlying Cd tolerance and accumulation in metallicolous populations have only been investigated in Auby (50°24′23.91″N, 03°04′56.38″E) and Langelsheim (51°56′34.08″N, 10°20′56.40″E) populations from the northwestern (NW) GU (Talke *et al.*, 2006; Weber *et al.*, 2006; Courbot *et al.*, 2007; Hanikenne *et al.*, 2008; Willems *et al.*, 2010; Baliardini *et al.*, 2015).

In this work, we compared the ionomes, transcriptomes and metabolomes of two *A. halleri* metallicolous populations from two different genetic units (GUs): PL22, from the hybrid zone (HZ) GU (in southern Poland), and I16, from the southeastern (SE) GU (in northern Italy), which were chosen for their contrasting Cd accumulation profiles (Meyer *et al.*, 2015). Our results indicate that PL22 and I16 have evolved two contrasting strategies of Cd tolerance leading to either hyperaccumulation or limited accumulation of Cd both in roots and shoots. Results also suggest the importance of flavonoid accumulation to cope with Cd toxicity.

Materials and Methods

Seeds, soil and plant material

Arabidopsis halleri ssp. *halleri* (Linnaeus) O'Kane & Al-Shehbaz PL22 and I16 plants (Meyer *et al.*, 2015) and seeds were harvested in the south of Poland (Bukowno) and in the north of Italy (Val del Riso). The PL22 population belongs to the HZ GU, while I16 belongs to the SE GU (Pauwels *et al.*, 2012; Supporting Information Fig. S1a,b). PL22 and I16 plants, seeds and soil samples were collected *in situ*, respectively, in September and July 2015. Shoots were harvested from eight plants. Soil (200 g DW per sample), close to each harvested plant, was collected at 10–20 cm from the rim of the hole after digging out the plants with their root systems. Soil samples were collected at 0–15 cm soil depth, which corresponds to the growth zone of *A. halleri* roots.

Physicochemical analysis and metal quantification in field samples

Sample digestion and mineral element quantification of PL22 and I16 shoots and soil collected *in situ* were performed according to Houba *et al.* (1986), Pueyo *et al.* (2004) and Menzies *et al.* (2007). More detailed information about mineral element quantification, and pH and electrical conductivity (EC) measurements in soil are reported in Methods S1.

Experimental design of hydroponic culture with *A. halleri* populations

PL22 (HZ) and I16 (SE) seeds were sown on vermiculite in a controlled growth chamber (16 h light d^{-1}; 100 µmol photons m^{-2} s^{-1} irradiance; 20°C : 18°C, day : night, and 70% humidity). After 4 wk of growth, plants were transferred to 4-l vessels filled with a modified Murashige and Skoog (MS) solution and placed in a glasshouse (100 µmol photons m^{-2} s^{-1} irradiance) (Meyer *et al.*, 2015). Vessels were randomly distributed and moved around once a week during the change of nutrient solution.

After 4 wk in nutrient solution, 90 plants for each population were chosen for the growth test. Half of the plants (45 individuals) were transferred to vessels containing 5 µM $CdSO_4$ (as in Meyer *et al.*, 2015), while the others were kept in the control solution (Fig. S2).

After 10 d, roots and shoots from each plant were harvested separately, weighted and washed three times (for 10 min) with 0.5 mM $CaCl_2$. Roots and shoots from each population were then divided into three biological replicates (15 plants per replicate), ground in liquid nitrogen and kept at −80°C for ionomic, transcriptomic and metabolomic analyses.

Physiological and ionomic analysis of samples grown hydroponically

Relative chlorophyll content (CCM-200 chlorophyll meter; Opti-Sciences, Hudson, NH, USA) and shoot area (two measurements per plant) were recorded from 15–25 plants for each population and condition at 0, 3, 6 and 10 d after stress initiation (Fig. 1).

For mineral analysis, 1 g from each biological replicate was measured and dried at 37°C until constant weight. The mineral profile of all samples was determined by inductively coupled plasma mass spectrometry (as in Meyer *et al.*, 2015).

RNA extraction and mRNA sequencing (mRNA-Seq) analysis

Total RNA was extracted from 100 mg of ground-frozen root and shoots samples using the Maxwell® LEV Plant RNA Kit (Promega, Madison, WI, USA). RNA was quantified with the NanoDrop 2000 UV-Vis Spectrophotometer (Thermo Scientific, Loughborough, UK). Libraries were prepared with the TruSeq Stranded mRNA Library Prep Kit (Illumina, San Diego, CA, USA) and sequenced in four runs with an Illumina NextSeq500 device yielding on average 35 million reads per sample. Transcript

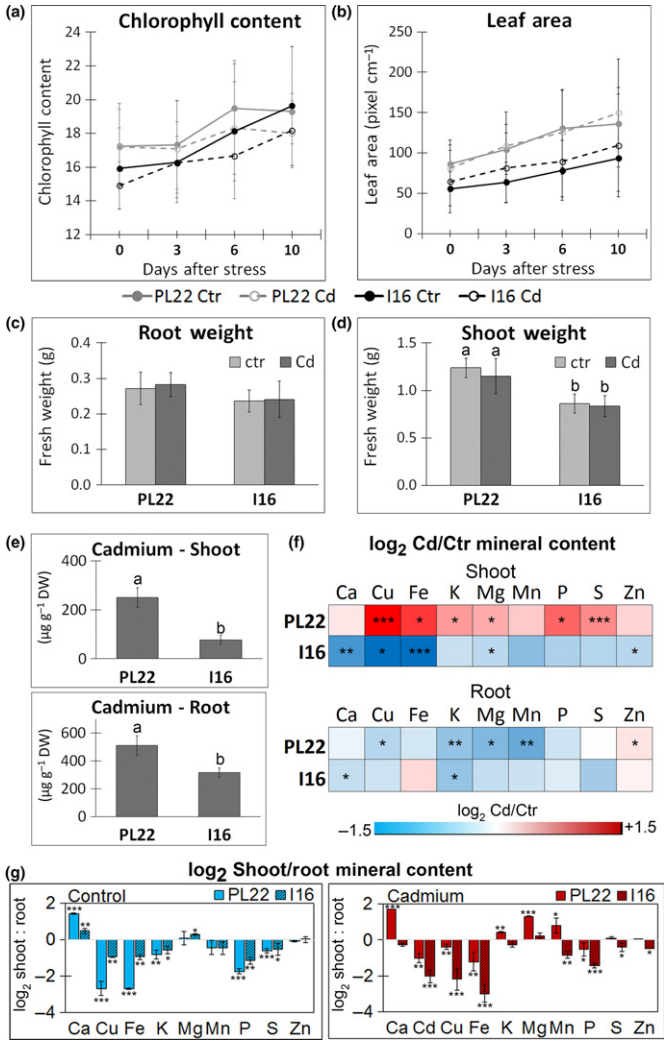

Fig. 1 Physiological analysis and mineral element quantification in control (Ctr) and cadmium (Cd)-treated *Arabidopsis halleri* plants. (a) Chlorophyll content, (b) leaf area, and (c) root and (d) shoot weights were measured in Ctr and Cd-treated plants. Error bars represent ± SD ($n = 25$–30). (e) Cd concentration in PL22 and I16 Cd-treated roots and shoots (three biological replicates) measured after 10 d in hydroponic solution containing 5 μM $CdSO_4$. (f, g) Heat maps representing (f) $\log_2$ Cd : Ctr and (g) $\log_2$ shoot : root ratio of essential mineral element concentrations in PL22 and I16 plants (three biological replicates). Red and blue indicate higher and lower (mineral element), respectively, in Cd samples with respect to Ctr (f). Different letters indicate statistically significant differences ($P = 0.05$) by ANOVA with Tukey's range test. Asterisks indicate statistically significant differences (*, $P < 0.05$; **, $P < 0.01$; ***, $P < 0.001$) assessed using a *t*-test.

abundance estimation was carried out by mapping the reads of each sample to a reference transcriptome of *A. halleri* (PL22; 34.829 annotated transcripts with an average length of 1.256 bp and N50 equal to 1.675 bp; Schvartzman *et al.*, 2017) with the align_and_estimate_abundance.pl perl script from Trinity (Broad Institute, Cambridge, UK; Hebrew University of Jerusalem, Jerusalem). The algorithms used for alignment and abundance estimation were Bowtie2 and Rsem, respectively. The RNA sequencing (RNA-Seq) reads and transcriptome assembly have been deposited at the National Center for Biotechnology Information Transcriptome Shotgun Assembly Sequence Database (TSA) with BioProject identification number PRJNA388549.

Statistical analysis, data mining and gene ontology enrichment analyses of RNA-Seq data

Statistical analyses to identify differentially expressed genes (DEGs) were performed using the DEseq2 R package (Love *et al.*, 2014). Two pairwise comparisons using PL22 and I16 RNA-Seq counts were carried out; the thresholds for selecting DEGs were $\log_2$ fold change (FC) > 0.5 and < −0.5 and false discovery rate (FDR) < 0.05. The aim of the first comparison was evaluation of the individual effects of the GU (comparison of DEGs for PL22 vs I16) in control and Cd-treated samples (three control + three Cd-treated samples for each population) on gene expression separately in the root and shoot. To evaluate the effect of the treatment (Cd and control) in each population, a second pairwise comparison was performed between Cd and control samples separately for PL22 and I16 roots and shoots (e.g. PL22 Cd-treated vs PL22 control shoot samples). This method evaluates the weight of each comparison considered in the analysis and its impact on DEGs. Gene ontology (GO) enrichment analyses were performed for each set of genes induced in PL22 ($\log_2$ PL22/I16 > 0.5) or I16 ($\log_2$ PL22/I16 < −0.5) using the BiNGO tool (Maere *et al.*, 2005) with the built-in Fisher's exact test function (FDR < 0.05).

Heat map and hierarchical clustering analyses of mRNA-Seq data were carried out using the 'heatmap.2' function (gplots R package). Expression values used for the analysis were filtered based on the median value.

Principal component analysis (PCA) was carried out and related graphs generated using the prcomp and scatterplot3d R packages, respectively.

cDNA synthesis and qRT-PCR analysis

Quantitative reverse transcription–polymerase chain reaction (qRT-PCR) analyses were carried out according to Baliardini *et al.* (2016). Primers for qRT-PCR are listed in Table S1 and more detailed information is reported in Methods S1.

Metabolomic analysis

Two hundred milligrams of frozen homogenized powder was resuspended with 1 volume (w/v) of liquid chromatography–mass spectrometry (LC-MS)-grade MilliQ water (Merck, Overijse, Belgium) and then mixed with 10 volumes (w/v) of glacial chloroform : methanol (2 : 1). The samples were vortexed for 30 s, stored on ice for 1 h, sonicated for 15 min and centrifuged (25 min at 4500 ***g*** and 4°C). The methanolic phases were recovered, diluted 1 : 1 in LC-MS-grade MilliQ water, passed through 0.2-μm Minisart RC4 filters (Sartorius-Stedim Biotech, Göttingen, Germany) and analysed by reversed-phase high-performance liquid chromatography (RP-HPLC) using a Gold 127 HPLC System (Beckman Coulter,

Brea, CA, USA), a C18 guard column (7.5 × 2.1 mm; 5 µm particle size) and an Alltech (Nicholasville, KT, USA) RP C18 column (150 × 2.1 mm; 3 µm particle size). A gradient between solvent A (0.5% formic acid and 5% acetonitrile in water) and solvent B (100% acetonitrile) was established as follows: 0–10% B in 2 min, 10–20% B in 10 min, 20–25% B in 2 min, 25–70% B in 7 min, isocratic for 5 min, 70–90% B in 1 min, isocratic for 14 min, 90–100% B in 1 min and 20 min of equilibration. For each sample, 10 µl was injected at a flow rate of 0.2 ml min^{-1}.

The HPLC instrument was coupled to an ion trap mass spectrometer equipped with an electrospray ionization (ESI) source (Esquire 6000; Bruker Daltonik, Bremen, Germany). Mass spectra were recorded in alternating positive and negative ionization mode within the range 50–2000 *m/z* with a target mass of 400 *m/z*. Nitrogen was used as the nebulizing gas (50 psi; 350°C) and drying gas (10 l min^{-1}) and the vacuum pressure was 1.4×10^{-8} bar. For fragmentation analysis, MS/MS and MS^3 spectra were recorded in positive and negative ionization modes in the range 50–2000 *m/z*. Helium was used for collision-induced dissociation (amplitude = 1 V). MS data were recorded using Esquire control v.5.2 software and processed using Esquire data analysis v.3.2 software (Bruker Daltonik).

Metabolites were identified by comparing retention times, *m/z* values and fragmentation patterns with those of commercial standards, an in-house library, online databases (MassBank; www.massbank.jp) and the scientific literature (Morreel *et al.*, 2014). Neutral losses of 132, 146 and 162 Da were considered diagnostic of the loss of pentose, deoxyhexose and hexose sugars, respectively.

Chromatograms were converted to netCDF files for peak alignment and peak area extraction using MZmine software (http://mzmine.github.io/).

Glutathione and ascorbic acid measurements

Total and oxidized glutathione was measured using the GSH-Glo™ Glutathione Assay (Promega), using 50 mg of PL22 and I16 shoot samples ground in liquid nitrogen and following the manufacturer's instructions.

Ascorbic acid (AA) was measured using a method adapted from Davey *et al.* (2003) (Methods S1).

Mutant selection and growth tests

Arabidopsis thaliana (thale cress) wild-type (WT) and transgenic lines were in the Columbia-0 (Col-0) background. The T-DNA insertion mutants of *FLAVANONE 3-HYDROXYLASE* (*F3H*) (SALK_113904) and *FLAVONOL SYNTHASE 1* (*FLS1*) (SALK_076420) were kindly provided by Prof. Brenda Winkel (Department of Biological Science, VirginiaTech, Blacksburg, VA, USA; Bowerman *et al.*, 2012), *transparent testa 8* (*tt8*) (SALK_082999) seeds were provided by Prof. Song Susheng (Tsinghua-Peking Center for Life Sciences, MOE Key Laboratory of Bioinformatics, Tsinghua University, Beijing, China; Qi *et al.*, 2011) and *cyclic nucleotide gate channel 12* (*cngc12*) knockout (ko) mutants were provided by Prof. Keiko Yoshioka (Department of Cell & Systems Biology, University of Toronto, Toronto, Canada; DeFalco *et al.*, 2016). Finally, T-DNA insertion mutants of *VACUOLAR MEMBRANE ATPAse 10* (*VMA10*) (CS473188) and *CYCLIC NUCLEOTIDE GATE CHANNEL 3* (*CNGC3*) (SALK_056832; Gobert *et al.*, 2006) were obtained from GABI-kat (Center for Biotechnology and Department of Biology, Bielefeld University, Bielefeld, Germany) or Nottingham Arabidopsis Stock Centre (NASC, University of Nottingham, Nottingham, UK). In order to obtain seeds and plant material for genotyping, WT and mutants were grown in soil in a growth chamber under a short-day photoperiod (8 h : 16 h, light : dark period; 70% relative humidity) at a light intensity of 100 µmol for 4 wk. Then plants were transferred to a growth chamber with a long-day photoperiod (16 h : 8 h, light : dark period; 100 µmol light intensity; light, 60% relative humidity and 22°C; dark, 70% relative humidity and 20°C).

For *in vitro* growth, seeds were sterilized in 70% ethanol for 3 min and in 5% (v/v) bleach : 0.1% (v/v) sodium dodecyl sulfate for 5 min and then rinsed three times with sterile water. Thereafter, seeds were sown onto square Petri plates containing half-strength MS (MS/2) medium containing 1% sucrose, 0.05% 2-(N-morpholino) ethanesulfonic acid and 0.8% agar, and stratified at 4°C for 72 h. Plants were cultivated in a growth chamber (16 h 23°C : 8 h 18°C, light : dark; 150 µmol light intensity), vertically oriented for the root growth test, or horizontally oriented for antibiotic selection.

For the growth test, *A. thaliana* WT and ko plantlets were grown on MS/2 agar medium for 7 d. Thereafter, half of the plants were maintained on the control medium, and the others were transferred to MS/2 agar medium supplemented with 100 µM $CdCl_2$. Primary and lateral root length were analysed using RootNav software (Pound *et al.*, 2013), shoot area was measured with Fiji software (Schindelin *et al.*, 2012) and chlorophyll content was measured as in Warren (2008).

Statistical analysis of physiological, ionomic and metabolomic data

To assess statistical differences in physiological parameters (chlorophyll content, growth and weight) and mineral element concentration among *A. halleri* populations, a *t*-test (Cd vs control or shoot vs root) and ANOVA (differences among populations) with Tukey's range test ($P = 0.05$) were performed using the agricolae R package.

Root growth and shoot area for *A. thaliana* ko mutants after Cd contamination treatment were normalized using the control ($\frac{\text{Cd sample growth}}{\text{Ctr sample growth}}$), then statistically compared with the WT values in the Cd treatment ($\% \frac{\text{Mutant growth}}{\text{WT growth}}$). In order to evaluate statistical differences for root and shoot growth between WT and mutants, ANOVA with Tukey's range test ($P = 0.05$) was performed using the agricolae R package.

Results

Soil and shoot mineral profiles of two *A. halleri* metallicolous populations from a field survey

To characterize the *A. halleri* plants grown in their native sites, mineral element profiles of PL22 and I16 shoots, and of Bukowno (PL22 site) and Val del Riso (I16 site) soil samples were collected and analysed, as well as soil pH and EC (Fig. S1c–f). Interestingly, Cd concentrations in shoots and soil showed an opposite trend between the two metallicolous populations (Fig. S1c). Specifically, PL22 accumulated four-fold higher Cd concentrations in the shoot with respect to I16 (208 and 59 mg kg^{-1} DW in PL22 and I16, respectively). Conversely, I16 native soil was characterized by a three times higher Cd content compared with PL22 soil (0.7 and 2.5 mg kg^{-1} DW in PL22 and I16 soil, respectively). It is worth mentioning that the bioaccumulation factor for Cd, that is, the ratio between the shoot Cd content and the 0.01 M $CaCl_2$-extractable Cd content in soil, was 282 in PL22 and 24 in I16. A similar trend was observed for Zn (Fig. S1d–f). pH and EC in soils collected at PL22 and I16 sites were similar.

The two metallicolous populations showed similar tolerance levels but contrasting Cd accumulation and mineral profile

In order to assess intraspecific variability in Cd accumulation and tolerance, a growth test in hydroponic culture was performed. After 4 wk of growth in vermiculite and 4 wk of acclimatization in hydroponic control solution, plants were subjected to a 5 μM Cd contamination (as in Meyer *et al.*, 2015) for 10 d, which corresponds to a realistic concentration (0.6 ppm; Fig. S1c). Measurements of chlorophyll content (Fig. 1a), leaf area (Fig. 1b), and root and shoot biomasses (Fig. 1c,d) supported the absence of Cd toxicity symptoms for both populations. However, PL22 plants showed higher shoot and root biomasses than I16.

Both shoots and roots of PL22 plants accumulated significantly higher Cd concentrations than I16, which behaved as an excluder with limited Cd accumulation in roots and transfer to shoots (Fig. 1e). Furthermore, PL22 roots were characterized by significantly decreased copper (Cu), potassium (K), magnesium (Mg) and manganese (Mn) concentrations after Cd treatment, while Zn concentration increased. In contrast, Cu, Fe, K, Mg, phosphorus (P) and sulphur (S) concentrations significantly increased in PL22 shoots upon exposure to Cd (Fig. 1f). I16 showed the opposite behaviour to PL22, with lower concentrations of calcium (Ca), Cu, Fe, Mg and Zn concentrations in Cd-treated shoots compared with the control shoots and minor changes in root mineral profile. Globally lower shoot : root ratios were observed for all the mineral elements analysed in I16 Cd-treated samples with respect to PL22 (Fig. 1g).

Taken together, these results indicate contrasting strategies of adaptation to Cd exposure by I16 and PL22 populations.

Global transcriptomics analysis

Roots and shoots were harvested in control and 5 μM Cd-contaminated conditions and subjected to RNA-Seq analysis (Fig. 2a; Table S2). To confirm the quality of the transcriptome *de novo* assembly and RNA-Seq data (see the Materials and Methods section, and Schvartzman *et al.*, 2017), the expression patterns of 20 key genes were validated in PL22 and I16 shoot and root samples by qRT-PCR (Fig. S3a). Results showed that the RNA-Seq and qRT-PCR expression profiles of selected genes were strongly correlated ($r = 0.92$; FDR < 2.2 E^{-16}).

First, the impact of the GU (PL22 vs I16) and the treatment within each population (e.g. Cd vs control in PL22) on DEGs was estimated by pairwise analysis (Fig. 2a). The PCA conducted on RNA-Seq data highlighted the GU as the factor having the strongest impact on gene expression profiles (Fig. 2b). PL22 and I16 samples are separated according to the GU by the first principal component (PC1), accounting for 55% and 61% of the variance in the root and shoot, respectively. The 'treatment' factor (PC2) showed a lower impact on the number of DEGs (Table S2), accounting for 26% and 22% of the variance in the root and shoot, respectively. Indeed, a small number of DEGs were modulated by Cd treatment in each population and the majority of these genes were downregulated by Cd (Fig. 2a). Interestingly, most DEGs were identified in the root.

A GO term enrichment analysis was conducted with DEGs that had higher expression in one population than the other (Fig. 2a). Given that Cd treatment had a limited effect on gene expression in both populations (Fig. 2a), the GO enrichment analysis was carried out with Cd and control DEGs together (six replicates for each population). In shoots, a striking number of genes related to secondary metabolism, phenylpropanoids and glutathione, in particular, had significantly higher expression in PL22 than in I16 (Table S3). Enrichment analysis conducted on I16 DEGs highlighted an enrichment of 'cell wall' GOs in both the root and shoot (Table S3).

Taking into account ionomic and GO enrichment analyses of RNA-Seq data, we focused our attention on genes with a role in transport and secondary metabolism. These genes were further divided into two main categories: DEGs with significantly higher (or lower) expression in PL22 than I16 regardless of the treatment, and DEGs with significantly higher (or lower) expression in PL22 than I16 and whose expression was significantly modulated by Cd treatment (e.g. the intersection between 'Genes with higher expression in PL22 than I16' and 'Genes modulated by Cd in PL22' in Fig. 2a).

Among the genes that had higher expression in PL22 roots and are involved in transport (Figs 3a, 4), most showed constitutively higher expression compared with I16 (Figs 3a, S3a; Table S4), such as *IRT1*, *CATION EXCHANGER 4* (*CAX4*), *YELLOW STRIPE like 3* (*YSL3*) and *CNGC12*, while others were significantly induced by Cd treatment in PL22 (e.g. *OLIGOPEPTIDE TRANSPORTER 3* (*OPT3*), *ZINC INDUCED FACILITATOR 1* (*ZIF1*) and *CNGC3*; Figs 3a, 4a, S3). In the genes that had higher expression in I16 than in PL22 and are involved in

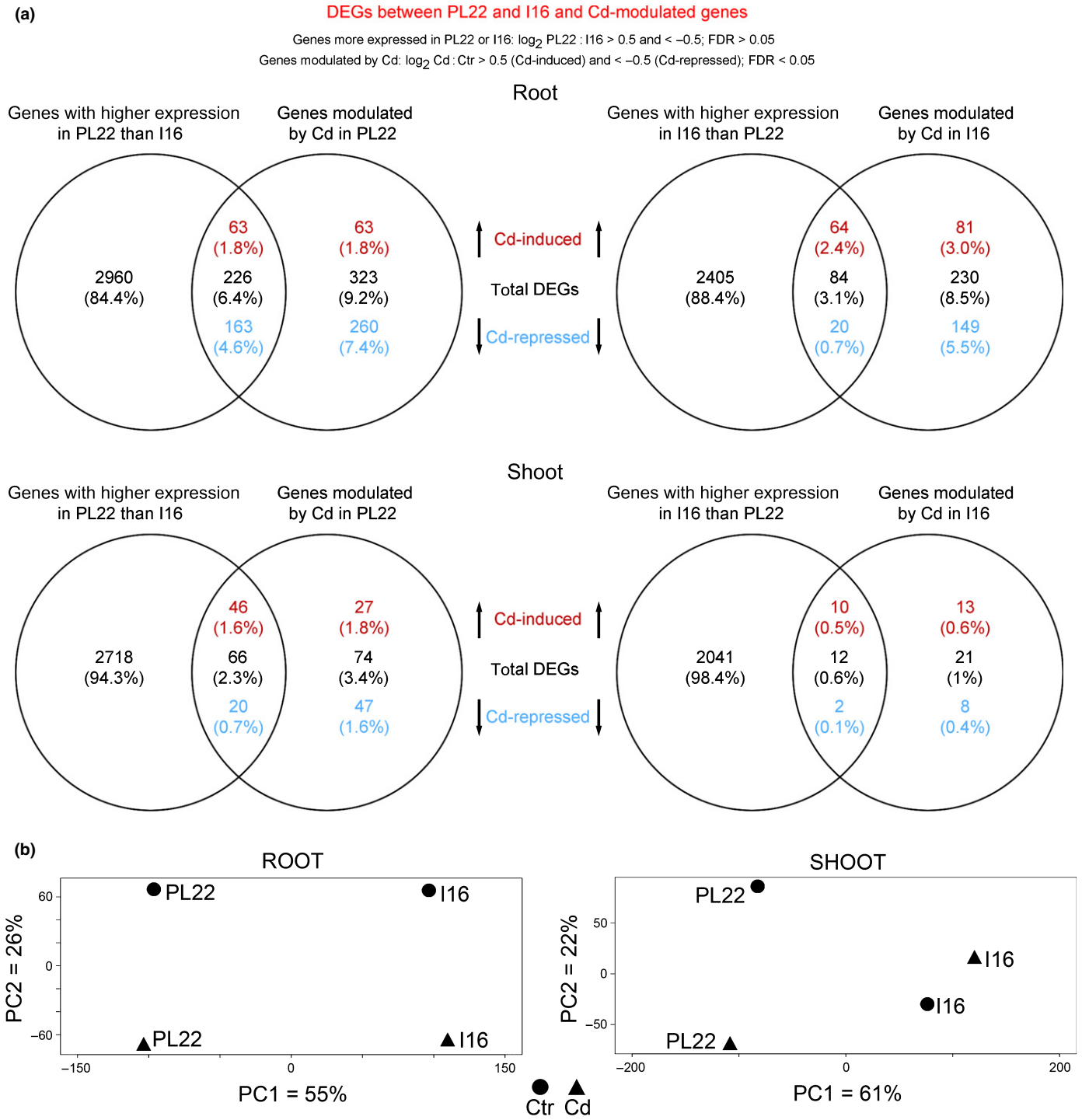

Fig. 2 Differentially expressed genes (DEGs) and principal component (PC) analysis in *Arabidopsis halleri* PL22 and I16 roots and shoots. (a) Pairwise comparison between PL22 and I16 RNA sequencing (RNA-Seq) data. The thresholds for selecting DEGs in PL22 vs I16 (i.e. three control (Ctr) + three cadmium (Cd)-treated samples for each population) were $\log_2$ PL22 : I16 counts > 0.5 (genes with higher expression in PL22 than I16) and < −0.5 (genes with higher expression in I16 than PL22). DEGs induced ($\log_2$ Cd : Ctr > 0.5) or repressed ($\log_2$ Cd : Ctr < −0.5) by Cd treatment are also shown. (b) PL22 and I16 sample distribution in roots and shoots according to PC1 and PC2. The percentage of variance is reported for each component.

transport (Figs 3a, 4a; Table S4), the majority showed constitutive differences in expression (e.g. *NITRATE TRANSPORTER 1.5* (*NRT1.5*), *NRT1.5-like*, *NRT3.1* and *BASIC-LEUCINE ZIPPER 6* (*ZIP6*)) and many were further induced by Cd, such as *FERRIC REDUCTASE DEFECTIVE 3* (*FRD3*) and *SLAC1 HOMOLOGUE 1* (*SLAH1*). As suggested by GO enrichment analysis, most of the root cell wall-related DEGs (Table S4e,f), showed constitutively higher expression in I16 (154 DEGs) than in PL22 (69 DEGs), and only a few of them were significantly modulated by Cd (10 DEGs in I16 and seven DEGs in PL22).

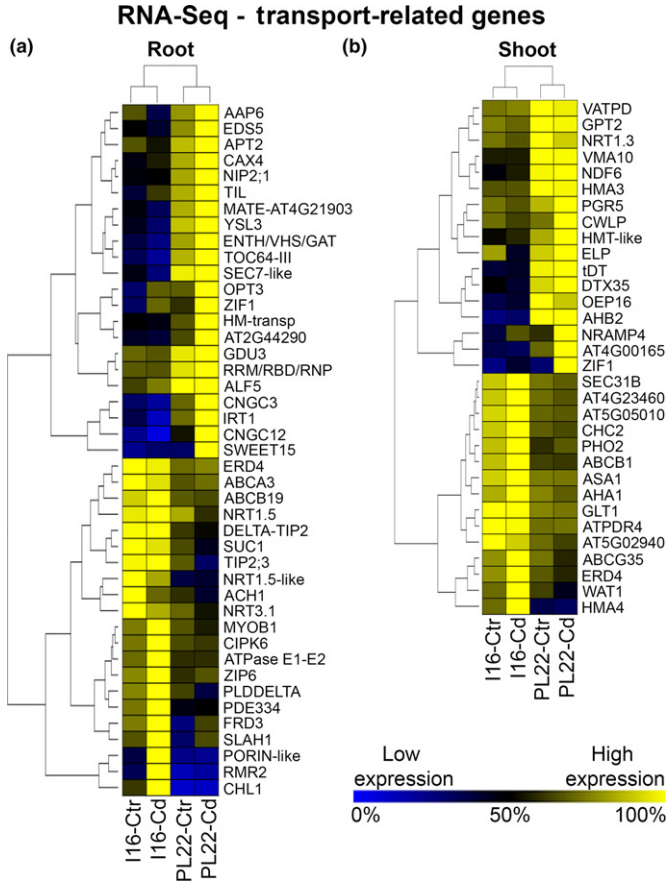

Fig. 3 Expression of transport-related genes in *Arabidopsis halleri* PL22 and I16. (a, b) Heat map showing the RNA sequencing (RNA-Seq) expression of transport-related genes that showed higher expression in PL22 ($\log_2$ PL22 : I16 > 0.5) and I16 ($\log_2$ PL22 : I16 < −0.5) (a) roots and (b) shoots. The expression values were calculated as a percentage related to the sample showing the highest expression value for each gene (100% and 0% for yellow and blue colours, respectively) within PL22 and I16 (control (Ctr) and cadmium (Cd)). Gene names are also reported.

Similarly to roots, the majority of differentially expressed (DE) transporter genes in control conditions showed higher expression in PL22 than in I16 shoots (Fig. 3b; Table S4), and *NATURAL RESISTANCE ASSOCIATED MACROPHAGE PROTEIN 4* and *ZIF1* were further induced by Cd treatment (Figs 3b, 4b; Table S4). Interestingly, in I16, *HMA4* showed constitutively higher expression compared with PL22 (Figs 4a, S3b). Furthermore, a striking number of genes involved in flavonoid biosynthesis (*PHENYLALANINE AMMONIA-LYASE 1* (*PAL1*), *CHALCONE SYNTHASE* (*CHS*), *CHALCONE FLAVONONE ISOMERASE* (*CHI*), *DIHYDROFLAVONOL 4-REDUCTASE* (*DFR*), *LEUCOANTHOCYANIDIN DOOXYGENASE* (*LDOX*), *FLAVONONE 3-HYDROXYLASE* (*F3H*), *FLAVONAL SYNTHASE 1* (*FLS1*), *ANTHOCYANIDIN REDUCTASE* (*ANR*), *UDP-GLUCOSE:FLAVONOID 3-O-GLUCOSYLTRANSFERASE* (*UFGT*), *4-COUMARATE:COEENZYME A LIGASE* (*4CL*)), signal transduction (*TRANSPARENT TESTA 8* (*TT8*), *ELONGATED HYPOCOTYL 5* (*HY5*), *MYB DOMAIN PROTEIN 12* (*MYB12*)) and transport *DETOXIFYING EFFLUX CARRIER 35*, and of *GLUTATHIONE S-TRANSFERASE* (*GST*)-related genes were characterized by constitutively higher expression in PL22 compared with I16 shoots, as shown by the RNA-Seq data (Fig. 5a) and confirmed by qRT-PCR (Fig. S3b).

PL22 is characterized by high flavonoid and antioxidant contents

The RNA-Seq data clearly show upregulation and high expression of secondary metabolism-related genes in the PL22 shoot. To obtain a wider picture of these processes and to confirm the obtained results at the metabolite level, relative concentrations of flavonoids and hydroxycinnamic acids (HPLC-MS) in PL22 and I16 shoot samples were compared (Fig. 6; Table S5). As observed for RNA-Seq data (Fig. 2b), according to the PCA plot (Fig. 6a) of metabolite data (flavonoids and hydroxycinnamic acids), the sample distribution on PC1 (68% of variance) was mainly influenced by the GU, while treatment seemed to have a minor effect on metabolite accumulation (Fig. 6a). Sample distribution was confirmed by hierarchical clustering of a subset of data (only identified metabolites; unidentified metabolites were not considered), the signals of all the isotopes for each metabolite were summed (Table S5). Moreover, the heat map (Fig. 6b) highlighted flavonoids and hydroxycinnamic acids showing the greatest differences between I16 and PL22. Strikingly, the total flavonol (24 metabolites) content was 60% higher (Tukey's range test; $P < 0.05$) in PL22 than in I16, while the total content of hydroxycinnamic acids (13 metabolites) was higher in I16 (+55% compared with PL22; Fig. 6c). PL22 accumulated high relative contents of five glycosylated kaempferol-related metabolites and two glycosylated-quercetin flavonoids in both control and Cd-treated samples. These kaempferol and quercetin derivates are mainly conjugated to glucoside (glucose, Glu) and rhamnoside (rhamnose, Rha) substitutions. By contrast, the I16 population showed a higher accumulation of only one glycosylated kaempferol (Rha and arabinose substitutions) and of synapoyl malate (Fig. 6d). Moreover, total ascorbic acid (AA) content and the ratio between reduced (GSH) and oxidized (GSSG) glutathione, both indicators of the cellular redox state and antioxidant capacity, were both significantly higher in PL22 than in I16 shoots (Fig. 6e).

Genetic analysis in *A. thaliana* supports a role for flavonoids and newly identified transporter genes in Cd stress tolerance

We investigated the involvement of flavonoid (*F3H* and *FLS1*), transport-related (*CNGC3*, *CNGC12* and *VMA10*) and flavonoid transcription factor (*TT8*) genes showing higher expression in PL22 than in I16 by testing corresponding *A. thaliana* ko mutants. Several physiological parameters (primary and lateral root growth, shoot area and chlorophyll content) were measured (Fig. 7). No significant differences for growth parameters and chlorophyll content were noted in the control conditions between mutants and WT (Tukey's range test; $P < 0.05$; Fig. 7a,c), while reduced growth was observed in all mutants, except *fls1* for root growth, with respect to the WT when exposed to Cd stress (Fig. 7b,c).

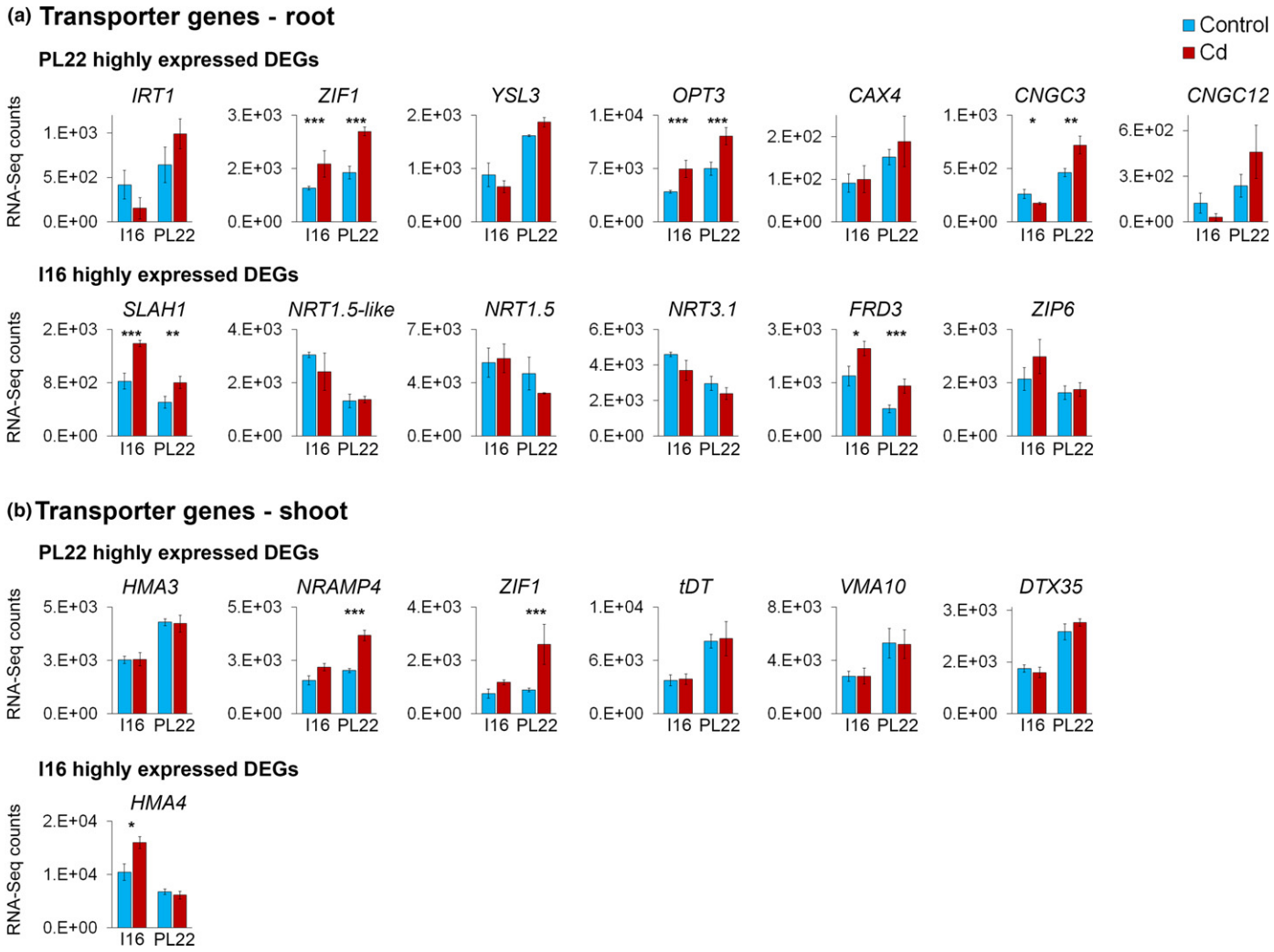

Fig. 4 RNA sequencing (RNA-Seq) expression of transporter genes with a putative role in the contrasting cadmium (Cd) accumulation strategies between PL22 and I16. (a, b) RNA-Seq expression data of transporter genes with higher expression in PL22 or I16 (a) roots and (b) shoots. Error bars represent ± SD. Asterisks indicate statistically significant differences between control and Cd treatment (*, $P < 0.05$; **, $P < 0.01$; ***, $P < 0.001$). DEGs, differentially expressed genes.

Discussion

We compared two *A. halleri* metallicolous populations from different European GUs, a hyperaccumulator-type (PL22) and an excluder-type (I16). In order to gain a better understanding of the different mechanisms involved in Cd tolerance and accumulation, the ionomes, transcriptomes and shoot metabolomes of PL22 and I16 were analysed under control and Cd-stress conditions.

PL22 and I16 showed contrasting Cd accumulation, mineral profiles and gene expression patterns

As showed in Meyer *et al.* (2015) and confirmed in this study (Fig. 1a–d), PL22 and I16 populations displayed similar high Cd and Zn (see Schvartzman *et al.*, 2017) tolerance levels. In their native site or hydroponically grown, PL22 hyperaccumulated Cd while I16 behaved as a Cd excluder. Hydroponically grown PL22 was also characterized by a global increase of essential elements in shoots (significant for Cu, Fe, K, Mg, P and S) during exposure to Cd and higher Ca, K, Mg and Mn shoot: root ratios in response to Cd treatment, which was in marked contrast to the behaviour of I16. These contrasting responses may be linked to a massive and nonspecific (Baxter & Dilkes, 2012) induction of transport-related pathways in PL22 reflecting its adaptation to Cd.

The analysis of transcriptomes showed that the GU was the main driver of gene expression differences, while Cd treatment had a small impact on the number of DEGs (Fig. 2a).

The good quality of the transcriptome is strongly supported by the high correlation between the RNA-Seq and qRT-PCR expression of several genes (Fig. S3) and the results obtained by Schvartzman *et al.* (2017).

Higher Cd accumulation in PL22 is paralleled by Cd-induced and constitutively high expression of transporter genes

Differences between the PL22 and I16 ionomic profiles (Fig. 1e–g) were to some extent reflected in the expression of transporter genes

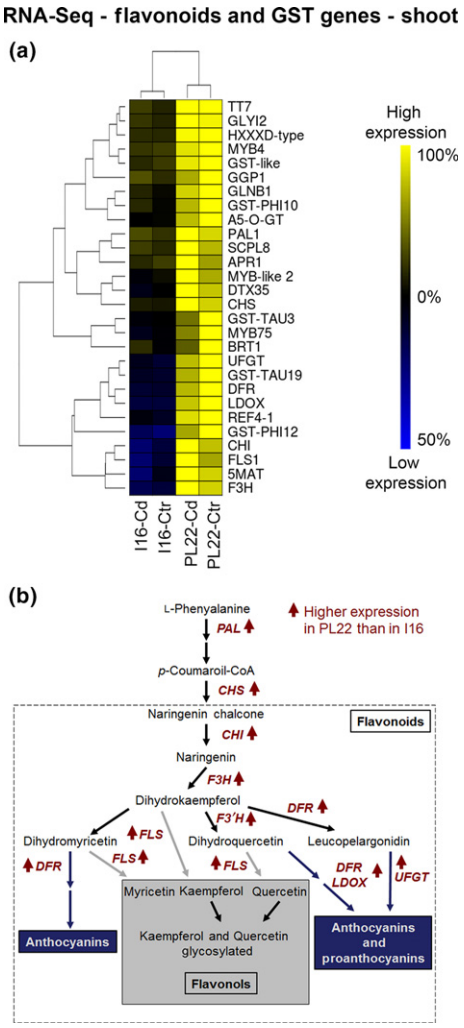

Fig. 5 Expression of flavonoids and *GLUTATHIONE S-TRANSFERASE* (*GST*) genes in PL22 and I16 shoots. (a) Heat maps showing the RNA sequencing (RNA-Seq) expression of flavonoid and GST genes with higher expression in PL22 than in I16 ($\log_2$ PL22 : I16 > 0.5). The expression values were calculated as a percentage related to the sample showing the highest expression value for each gene (100 and 0% for yellow and blue colours, respectively) within PL22 and I16 (control (Ctr) and cadmium (Cd)). Gene names are also reported. (b) Flavonoid biosynthetic genes showing constitutively higher expression in PL22 with respect to I16 shoots.

(Figs 3, 4). It is noteworthy that *IRT1*, the gene encoding the main Fe(II) transporter responsible for Cd uptake in the *A. thaliana* root (Vert *et al.*, 2002; Mendoza-Cózatl *et al.*, 2014) and probably in the Ganges hyperaccumulator population of *Noccaea caerulescens* (Plaza *et al.*, 2007), showed constitutively higher expression in PL22 roots compared with I16 (Fig. 4a; see also western blot analysis of IRT1 in Schvartzman *et al.*, 2017). IRT1 may be at least partially responsible for the higher Cd content in PL22 (Fig. 3a). Moreover, *OPT3* (Mendoza-Cózatl *et al.*, 2014; Zhai *et al.*, 2014) and *CAX4* (Mei *et al.*, 2009), genes that encode membrane transporters and are able to affect Cd transport, were found to have higher expression (*CAX4*) and to be induced by Cd treatment (*OPT3*) in PL22 compared with I16 roots (Fig. 4a).

In the shoot, *HMA3* (Morel *et al.*, 2009) also showed higher expression in PL22 than in I16 (Fig. 4b; Table S4). HMA3 was previously shown to play a pivotal role in Cd vacuolar sequestration in *A. thaliana* (Chao *et al.*, 2012) and in *N. caerulescens* (Ueno *et al.*, 2011). A role for HMA3 in leaf Cd hypertolerance and hyperaccumulation has not yet been demonstrated in *A. halleri*. However, high constitutive expression of *HMA3* was previously reported in *A. halleri* compared with *A. thaliana* (Becher *et al.*, 2004). Furthermore, high Cd vacuolar sequestration would provide an enhanced vacuolar sink for Cd, as already observed for *METAL TOLERANCE PROTEIN 1* and Zn root-to-shoot translocation (Gustin *et al.*, 2009).

Nicotianamine (NA) might also play a role in the contrasting accumulation observed between the two populations, as supported by the Cd-induced expression of the NA vacuolar transporter *ZIF1* (Haydon *et al.*, 2012) in PL22 roots and shoots (Figs 3a, 4a), and by the constitutive high expression of the metal-nicotianamine transporter *YSL3* (Waters *et al.*, 2006) in PL22 roots (Figs 3a, 4a). In strong support of this theory, Deinlein *et al.* (2012) showed that *A. halleri NICOTIANAMINE SYNTHASE 2* antisense lines with reduced NA content displayed reduced Cd translocation to and accumulation in the shoot. We cannot exclude at this stage the possibility that these genes also play a role in the higher shoot : root Cu ratio observed in PL22.

Among the genes that were not previously highlighted in transcriptomic analysis of metallophytes, *VMA10*, encoding the G1 subunit of the vacuolar (V) H^+-ATPase (Rouquié *et al.*, 1998), and the tonoplast malate dicarboxylate transporter gene *AhtDT* (Emmerlich *et al.*, 2003) showed higher expression in the shoots of the hyperaccumulating population (Fig. 4b). The latter is involved in vacuolar sequestration of malate, a well-known ligand for Zn in *A. halleri* (Sarret *et al.*, 2002). However, in contrast to the *vma10 A. thaliana* ko mutant, the *tDT* mutant did not show a Cd-sensitive phenotype (Fig. 7). *VMA10* is a component of the tonoplast-localized proton pump that provides energy for ion transport through vacuolar acidification (Sze *et al.*, 2002). As Cd tonoplast antiport activity in *A. thaliana* is dependent on an H^+ gradient mainly regulated by V-ATPase (Dietz *et al.*, 2001), we might speculate that there is a role for *AhVMA10* and *AtVMA10* in this processes. In strong support of this theory, Krebs *et al.* (2010) showed that an *A. thaliana* double mutant for the two tonoplast-localized isoforms of Vacuolar Proton ATPase exhibited reduced Zn tolerance, and Sambade *et al.* (2005) showed that yeast *vma* mutants were not able to grow in the presence of Zn. Furthermore, *AhCNGC3* and *AhCNGC12* (Fig. 4b) both showed higher expression in PL22 roots and *AhCNGC3* was further induced by Cd. The *cngc12* and *cngc3 A. thaliana* ko mutants displayed a striking growth reduction upon Cd treatment with respect to the WT (Fig. 7b). Previous characterization demonstrated that AtCNGC3 functions as a K uptake channel (Gobert *et al.*, 2006), while AtCNGC12 is a well-studied Ca transporter playing a role in stress responses (Urquhart *et al.*, 2011; DeFalco *et al.*, 2016). The induction of *AhCNGC3* by Cd treatment (Fig. 4b) was paralleled by the enhancement of root-to-shoot K transport in PL22 only in the presence of Cd (Fig. 1f,g), while

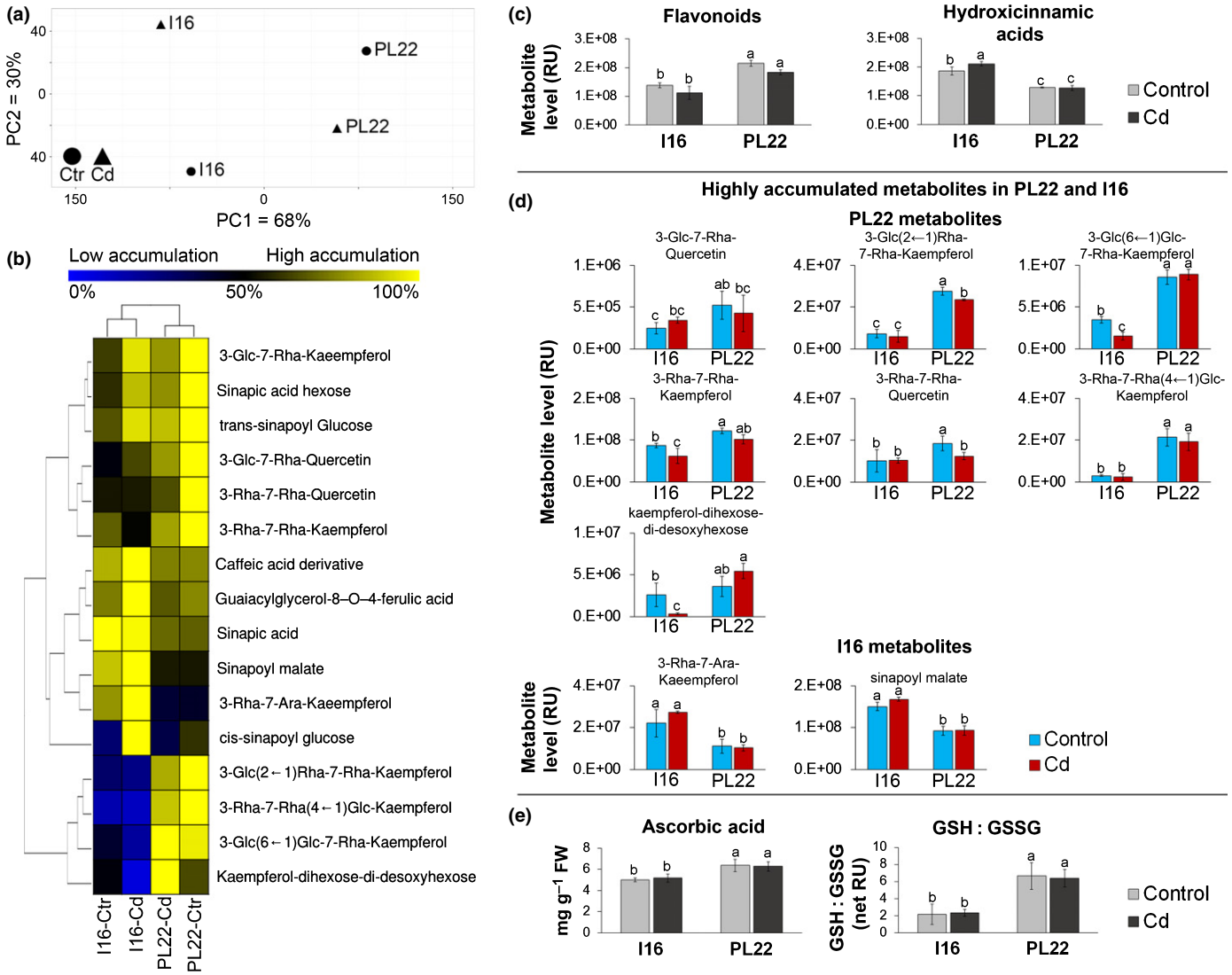

Fig. 6 Metabolomic analysis in *Arabidopsis halleri* PL22 and I16 shoots. (a) Principal component (PC) analysis of metabolomic data. PL22 and I16 sample distributions according to PC1 and PC2 are shown. The percentage of variance is reported for each component on the corresponding axes. (b) Heat map showing the flavonoid and hydroxycinnamic acid contents in PL22 and I16 shoots. The concentration values were calculated as a percentage related to the sample showing the highest value for each gene (100% and 0% for yellow and blue colours, respectively) within PL22 and I16 (control (Ctr) and cadmium (Cd)). (c, d) Quantification (relative units (RU)) of (c) total and (d) individual flavonoid and hydroxycinnamic acid metabolites with higher accumulation in PL22 ($\log_2$ PL22 : I16 > 0.5) or in I16 ($\log_2$ PL22 : I16 < −0.5) shoots. Error bars represent ± SD. (e) Ascorbic acid concentration and GSH : GSSG ratio in PL22 and I16 shoots. Different letters indicate statistically significant differences ($P = 0.05$) by ANOVA with Tukey's range test.

the high expression of *AhCNGC12* in control and Cd-treated PL22 roots (Fig. 4b) strikingly correlated with constitutive higher root-to-shoot Ca transport compared with I16 (Fig. 1g). This suggests that *CNGC3* and *CNGC12*, whose proteins in *A. thaliana* localized to the plasma membrane, may play a role in Cd-stress tolerance through the regulation of K and Ca cation homeostasis, respectively (Li *et al.*, 2012; Ahmad *et al.*, 2016). Ca and K have indeed a positive effect on the activity of antioxidant defence enzymes and decrease the content of H_2O_2 in plants treated with Cd (Ahmad *et al.*, 2016).

Thus, higher uptake of essential elements and of Cd in PL22 compared with I16 was supported by ionomic analysis (Fig. 1e,f) and RNA-Seq data (Figs 3, 4).

PL22 is characterized by constitutive high expression of flavonoid-related genes and high accumulation of flavonoids in shoots

The higher Cd uptake in roots, root-to-shoot translocation and accumulation in shoots observed in PL22 compared with I16 (Fig. 1e,g) are reflected in the activation of metabolic pathways involved in metal and ROS detoxification (Figs 5, 6). Identified candidates involved in those processes are flavonoid (kaempferol and quercetin glycosides in particular) and glutathione-S-transferase transcripts (Fig. 5a), as well as flavonoids and GSH metabolites (Fig. 6c–e), which had strikingly higher accumulation in PL22 than in I16 shoot

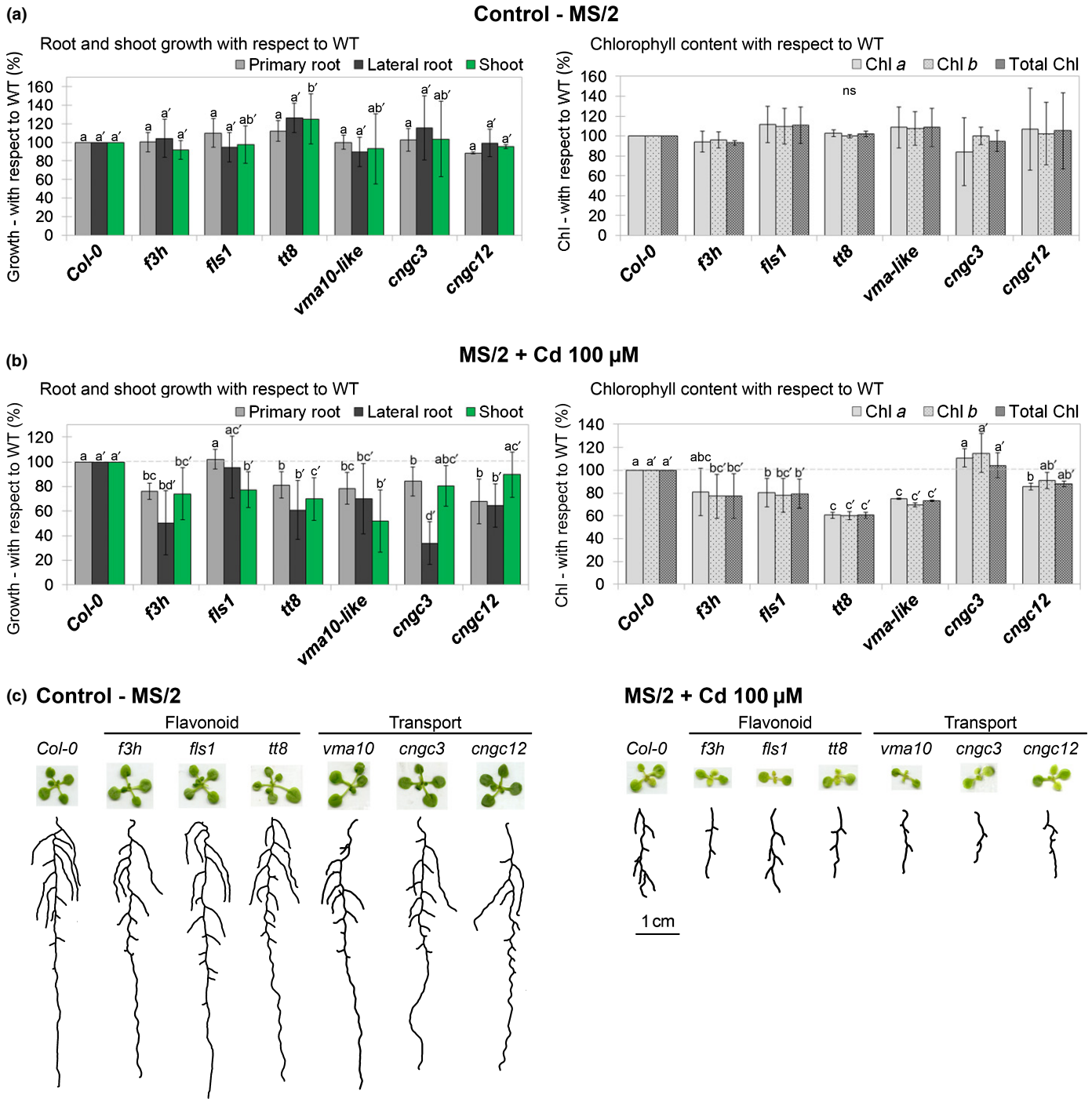

Fig. 7 *In vitro* growth test conducted in *Arabidopsis thaliana* Columbia (Col-0) wild-type (WT) and selected mutants grown in control and cadmium (Cd)-stress conditions. (a, b) Primary/lateral root length, shoot area and chlorophyll content were measured in (a) control and (b) 100 µM Cd treatment plants after 7 d of 100 µM Cd treatment. Error bars represent ± SD ($n = 15$; one representative experiment is shown). Different letters indicate statistically significant differences ($P = 0.05$) by ANOVA with Tukey's range test. (c) WT and mutant control and Cd-treated plants 7 d after Cd treatment. ns, not significant.

samples. The role of flavonoids in Cd tolerance and accumulation has been up to now poorly investigated in plants. Here we showed that *A. thaliana f3h*, *tt8* and, to some extent, *fls1* ko mutants were more sensitive to Cd stress with respect to WT (Fig. 7). Indeed, flavonoids, as well as glutathione and ascorbic acid, possess ROS-scavenging activity and they are capable of quenching H_2O_2 and oxygen free radicals (Agati *et al.*, 2012; Jozefczak *et al.*, 2014; Nakabayashi *et al.*, 2014), thus protecting cells from metal-induced oxidative damage. It is worth noting that plants subjected to different abiotic and biotic stresses showed a strong induction of flavonoid biosynthetic genes and an accumulation of their corresponding metabolites (Agati *et al.*, 2012; Nakabayashi *et al.*, 2014; Corso *et al.*, 2015). Interestingly, Cd stress upregulated the

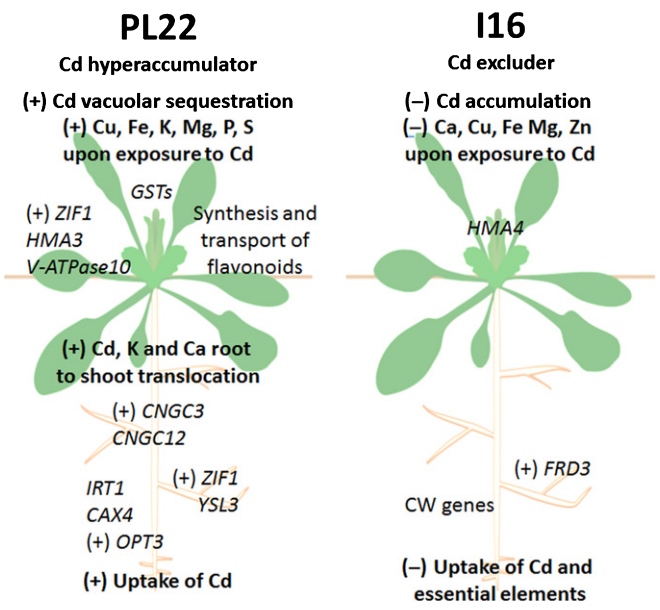

Fig. 8 Model summarizing differences in mechanisms of cadmium (Cd) resistance between *Arabidopsis halleri* PL22 and I16 populations. Genes differentially expressed between the PL22 and I16 populations related to mechanisms of Cd resistance are shown. (+) and (−) indicate regulation upon Cd exposure.

expression of transcripts involved in flavonoid biosynthesis in *A. thaliana* shoots (Herbette *et al.*, 2006) while no information is available in the literature about metabolite accumulation upon metal stresses and their potential role in metal distribution. In addition to the ROS-scavenging activity, direct metal binding may also contribute to reduced oxidative stress. Some flavonoids are indeed able to bind Fe, Cu and Cd *in vitro* (Fernandez *et al.*, 2002; Ravichandran *et al.*, 2014), and GSH plays a well-known dual role in Cd detoxification because of its high affinity for Cd and its being a precursor for phytochelatins (Jozefczak *et al.*, 2014).

Cd tolerance and accumulation are regulated by different pathways in PL22 and I16

In marked contrast to PL22, I16 was characterized by a reduction in the accumulation of essential elements (Ca, Cu, Fe, Mg and Zn) in the root and shoot upon Cd stress (Fig. 1f), as well as a lower Cd concentration. These responses may be related to reduced activation and expression of genes actively involved in the uptake and transport of such elements and to differences in cell wall composition between PL22 and I16 roots (Table S4e,f). The cell wall composition of different *A. halleri* populations (including PL22 and I16) was previously investigated using Fourier transform infrared spectroscopy (Meyer *et al.*, 2015). This technique allowed the identification of different spectra clearly associated with the I16 population (which was the only excluder) compared with the other tested populations but could not identify specific differences in the cell wall components, which needs further investigation.

Interestingly, *HMA4*, the heavy metal ATPase that plays a major role in root-to-shoot Zn/Cd translocation (Verret *et al.*, 2004; Courbot *et al.*, 2007; Hanikenne *et al.*, 2008), showed significantly higher expression in I16 shoots compared with PL22 shoots (Fig. 4b), while its expression was similar in PL22 and I16 roots. As in leaves *HMA4* is mainly expressed in mesophyll cells (Hanikenne *et al.*, 2008), its higher expression in I16 may help to exclude Cd from photosynthetically active tissues, as shown in *N. caerulescens* (Craciun *et al.*, 2012). Moreover, Siemianowski *et al.* (2014) showed that the ectopic expression of *AtHMA4* in *Nicotiana benthamiana* shoots reduced Cd uptake/accumulation and the concentration of other elements (e.g. Cu and Zn). Recently, a study of three Cd-hyperaccumulating populations of *Noccaea brachypetala* also showed that the highest shoot *HMA4* expression was found in the least Cd-accumulating population (Martos *et al.*, 2016). In this light, the higher expression of *HMA4* in the I16 shoot may also be consistent with the differences observed in the ionomic profiles.

Constitutive higher expression in I16 compared with PL22 was observed at the root level for *NRT1.5* (Chen *et al.*, 2012), *NRT3.1* (Okamoto *et al.*, 2006) and *SLAH1* (Cubero-Font *et al.*, 2016), all of which play a role in root-to-shoot nitrate reallocation and stress responses. *AtNRT1.5* is involved in Cd root-to-shoot translocation and facilitate K loading into the xylem (Chen *et al.*, 2012; Li *et al.*, 2017), and *AtSLAH1* plays a pivotal role in the control of root/shoot NO_3^- and Cl^- transport (Cubero-Font *et al.*, 2016). In this context, Cd transport and tolerance mechanisms may be regulated by NO_3^--dependent mechanisms in the I16 population. Alternatively, we cannot exclude the possibility that the higher expression of *NRT1.5*, *NRT3.1* and *SLAH1* in I16 is independent of adaptation to Cd contamination. *FRD3* also showed higher expression and was induced by Cd in I16 roots. *FRD3*, encoding a citrate transporter, may be involved in the maintenance of Fe homeostasis during Cd treatment (Durrett *et al.*, 2007; Pineau *et al.*, 2012; Charlier *et al.*, 2015). Finally, lower activation of antioxidative defences and stress-related genes in I16 than in PL22 is probably attributable to the low Cd uptake and lower Cd accumulation in roots and shoot, respectively.

Towards a model for intraspecific variation of Cd hypertolerance and hyperaccumulation in *A. halleri*

This study provides a comprehensive description of the ionomic, transcriptomic and metabolomic responses in two contrasting metallicolous *A. halleri* populations from different GUs. A genetic analysis in *A. thaliana* indirectly supported the involvement of identified *A. halleri* genes in Cd tolerance (Fig. 7). Taken together, the results suggest that two divergent strategies for Cd uptake, transport and detoxification, have evolved in the PL22 and I16 metallicolous populations, driven by different genes and metabolic pathways (Fig. 8). In this light, the high Cd accumulation and tolerance observed in PL22 may be associated with the high expression of transporter genes affecting Cd uptake and transport in the root (*IRT1* in particular), root (*ZIF1*) and shoot (*ZIF1* and *YSL3*), the high Cd mobility and, in the shoot, Cd vacuolar sequestration (*HMA3*), the large increase of K and Ca root-to-shoot translocation upon Cd stress mediated by *CNGC3*

and *CNGC12*, respectively, and the high Cd detoxification by GST and flavonoid genes which may mediate antioxidant and/or Cd chelation responses. This indicates, as previously shown for Zn in *N. caerulescens* (Guimarães *et al.*, 2009), that hypertolerance in *A. halleri* is mainly controlled by the shoot, while higher accumulation is mainly controlled by the root. This work indicates that flavonoids may play an important evolutionary role in the adaptation of metallicolous populations though the enhancement of antioxidant capacity and/or Cd chelation in plants, which opens up new avenues for research.

I16 seems to have adapted to metal contamination mainly through a general limitation of entry of minerals to cells, which seems to involve the differential expression of cell wall genes and a different cell wall composition (Meyer *et al.*, 2015) in roots and shoots, lower *IRT1* expression in roots, higher *FRD3* expression in roots and higher *HMA4* expression in shoots (Fig. 8).

To summarize, this study demonstrates that *A. halleri* metallicolous populations from different GUs have evolved different mechanisms of adaptation to anthropogenic contamination.

Acknowledgements

The authors would like to thank Claire-Lyse Meyer who participated in initial discussions and helped with the hydroponic culture, Pietro Salis for technical support during the hydroponic experiment and Silvia Zaccaria for helping with *A. thaliana* mutants and with the qRT-PCR analysis. The authors are very grateful to Roman Ceroni, Mauro Abbadini and Erika Cabrini (Fattoria Ariete, Gorno, Italy) for their help with the collection of I16 plants and soils in Val del Riso (Italy). The authors also thank Prof. Brenda Winkel (Department of Biological Science, VirginiaTech, USA), Prof. Song Susheng (Tsinghua-Peking Centre for Life Sciences, MOE Key Laboratory of Bioinformatics, School of Life Sciences, Tsinghua University, Beijing, China) and Prof. Keiko Yoshioka (Department of Cell & Systems Biology, University of Toronto) for providing seeds of flavonoid and *CNGC12* ko mutants. This work was supported by the FNRS (grant PDR T.0206.13 to M.H. and N.V.) and the University of Liège (grant SFRD-12/03 to M.H.). M.H. is a Research Associate of the FNRS.

Author contributions

M.C., M.S.S., M.H. and N.V. designed the research. N.V. and M.H. directed the research. M.C., M.S.S., F.G., F.S. and E.M. performed the experiments. M.C. and M.S.S. analysed the data. M.C. generated all figures and Supporting Information. M.C. and N.V. wrote the paper, with comments from all authors.

References

Agati G, Azzarello E, Pollastri S, Tattini M. 2012. Flavonoids as antioxidants in plants: location and functional significance. *Plant Science* **196**: 67–76.

Ahmad P, Abdel Latef AA, Abd Allah EF, Hashem A, Sarwat M, Anjum NA, Gucel S. 2016. Calcium and potassium supplementation enhanced growth, osmolyte secondary metabolite production, and enzymatic antioxidant machinery in cadmium-exposed chickpea (*Cicer arietinum* L.). *Frontiers in Plant Science* **7**: 513.

Baliardini C, Corso M, Verbruggen N. 2016. Transcriptomic analysis supports the role of *CATION EXCHANGER 1* in cellular homeostasis and oxidative stress limitation during cadmium stress. *Plant Signaling & Behavior* **11**: e1183861.

Baliardini C, Meyer C-L, Salis P, Saumitou-Laprade P, Verbruggen N. 2015. *CATION EXCHANGER1* cosegregates with cadmium tolerance in the metal hyperaccumulator *Arabidopsis halleri* and plays a role in limiting oxidative stress in *Arabidopsis* spp. *Plant Physiology* **169**: 549–559.

Bashir K, Rasheed S, Kobayashi T, Seki M, Nishizawa NK. 2016. Regulating subcellular metal homeostasis: the key to crop improvement. *Frontiers in Plant Science* **7**: 1192.

Baxter I, Dilkes BP. 2012. Elemental profiles reflect plant adaptations to the environment. *Science* **336**: 1661–1663.

Becher M, Talke I, Krall L, Krämer U. 2004. Cross-species microarray transcript profiling reveals high constitutive expression of metal homeostasis genes in shoots of the zinc hyperaccumulator *Arabidopsis halleri*. *Plant Journal* **37**: 251–268.

Bowerman PA, Ramirez MV, Price MB, Helm RF, Winkel BS. 2012. Analysis of T-DNA alleles of flavonoid biosynthesis genes in *Arabidopsis* ecotype Columbia. *BMC Research Notes* **5**: 485.

Chao DY, Silva A, Baxter I, Huang YS, Nordborg M, Danku J, Lahner B, Yakubova E, Salt DE. 2012. Genome-wide association studies identify heavy metal ATPase3 as the primary determinant of natural variation in leaf cadmium in *Arabidopsis thaliana*. *PLoS Genetics* **8**: e1002923.

Charlier J-B, Polese C, Nouet C, Carnol M, Bosman B, Kramer U, Motte P, Hanikenne M. 2015. Zinc triggers a complex transcriptional and post-transcriptional regulation of the metal homeostasis gene *FRD3* in Arabidopsis relatives. *Journal of Experimental Botany* **66**: 3865–3878.

Chen C-Z, Lv X-F, Li J-Y, Yi H-Y, Gong J-M. 2012. Arabidopsis NRT1.5 is another essential component in the regulation of nitrate reallocation and stress tolerance. *Plant Physiology* **159**: 1582–1590.

Clemens S. 2017. How metal hyperaccumulating plants can advance Zn biofortification. *Plant and Soil* **411**: 111–120.

Corso M, Vannozzi A, Maza E, Vitulo N, Meggio F, Pitacco A, Telatin A, D'Angelo M, Feltrin E, Negri AS *et al.* 2015. Comprehensive transcript profiling of two grapevine rootstock genotypes contrasting in drought susceptibility links the phenylpropanoid pathway to enhanced tolerance. *Journal of Experimental Botany* **66**: 5739–5752.

Courbot M, Willems G, Motte P, Arvidsson S, Roosens N, Saumitou-Laprade P, Verbruggen N. 2007. A major quantitative trait locus for cadmium tolerance in *Arabidopsis halleri* colocalizes with *HMA4*, a gene encoding a heavy metal ATPase. *Plant Physiology* **144**: 1052–1065.

Craciun AR, Meyer C-L, Chen J, Roosens N, De Groodt R, Hilson P, Verbruggen N. 2012. Variation in *HMA4* gene copy number and expression among *Noccaea caerulescens* populations presenting different levels of Cd tolerance and accumulation. *Journal of Experimental Botany* **63**: 4179–4189.

Cubero-Font P, Maierhofer T, Jaslan J, Rosales MA, Espartero J, Díaz-Rueda P, Müller HM, Hürter A-L, Al-Rasheid KAS, Marten I *et al.* 2016. Silent S-type anion channel subunit SLAH1 gates SLAH3 open for chloride root-to-shoot translocation. *Current Biology* **26**: 2213–2220.

Davey MW, Dekempeneer E, Keulemans J. 2003. Rocket-powered high-performance liquid chromatographic analysis of plant ascorbate and glutathione. *Analytical Biochemistry* **316**: 74–81.

DeFalco TA, Marshall CB, Munro K, Kang H-G, Moeder W, Ikura M, Snedden WA, Yoshioka K. 2016. Multiple calmodulin-binding sites positively and negatively regulate Arabidopsis *CYCLIC NUCLEOTIDE-GATED CHANNEL12*. *Plant Cell* **28**: 1738–1751.

Deinlein WU, Weber M, Schmidt H, Rensch S, Trampczynska A, Hansen TH, Husted S, Schjoerring JK, Talke IN, Krä U *et al.* 2012. Elevated nicotianamine levels in *Arabidopsis halleri* roots play a key role in zinc hyperaccumulation. *Plant Cell* **24**: 708–723.

Dietz KJ, Tavakoli N, Kluge C, Mimura T, Sharma SS, Harris GC, Chardonnens AN, Golldack D. 2001. Significance of the V-type ATPase for the adaptation to stressful growth conditions and its regulation on the molecular and biochemical level. *Journal of Experimental Botany* **52**: 1969–1980.

Durrett TP, Gassmann W, Rogers EE. 2007. The FRD3-mediated efflux of citrate into the root vasculature is necessary for efficient iron translocation. *Plant Physiology* **144**: 197–205.

Emmerlich V, Linka N, Reinhold T, Hurth MA, Traub M, Martinoia E, Neuhaus HE. 2003. The plant homolog to the human sodium/dicarboxylic cotransporter is the vacuolar malate carrier. *Proceedings of the National Academy of Sciences, USA* **100**: 11122–11126.

Fernandez MT, Mira ML, Florêncio MH, Jennings KR. 2002. Iron and copper chelation by flavonoids: an electrospray mass spectrometry study. *Journal of Inorganic Biochemistry* **92**: 105–111.

Gobert A, Park G, Amtmann A, Sanders D, Maathuis FJM. 2006. *Arabidopsis thaliana* Cyclic Nucleotide Gated Channel 3 forms a non-selective ion transporter involved in germination and cation transport. *Journal of Experimental Botany* **57**: 791–800.

Guimarães MDA, Gustin JL, Salt DE. 2009. Reciprocal grafting separates the roles of the root and shoot in zinc hyperaccumulation in *Thlaspi caerulescens*. *New Phytologist* **184**: 323–329.

Gustin JL, Loureiro ME, Kim D, Na G, Tikhonova M, Salt DE. 2009. MTP1-dependent Zn sequestration into shoot vacuoles suggests dual roles in Zn tolerance and accumulation in Zn-hyperaccumulating plants. *Plant Journal* **57**: 1116–1127.

Hanikenne M, Nouet C. 2011. Metal hyperaccumulation and hypertolerance: a model for plant evolutionary genomics. *Current Opinion in Plant Biology* **14**: 252–259.

Hanikenne M, Talke IN, Haydon MJ, Lanz C, Nolte A, Motte P, Kroymann J, Weigel D, Krämer U. 2008. Evolution of metal hyperaccumulation required cis-regulatory changes and triplication of HMA4. *Nature* **453**: 391–395.

Haydon MJ, Kawachi M, Wirtz M, Hillmer S, Hell R, Krämer U. 2012. Vacuolar nicotianamine has critical and distinct roles under iron deficiency and for zinc sequestration in *Arabidopsis*. *Plant Cell* **24**: 724–737.

Herbette S, Taconnat L, Hugouvieux V, Piette L, Magniette M-LM, Cuine S, Auroy P, Richaud P, Forestier C, Bourguignon J *et al.* 2006. Genome-wide transcriptome profiling of the early cadmium response of *Arabidopsis* roots and shoots. *Biochimie* **88**: 1751–1765.

Houba VJG, Novozamsky I, Huybregts AWM, van der Lee JJ. 1986. Comparison of soil extractions by 0.01 M $CaCl_2$, by EUF and by some conventional extraction procedures. *Plant and Soil* **96**: 433–437.

Jozefczak M, Bohler S, Schat H, Horemans N, Guisez Y, Remans T, Vangronsveld J, Cuypers A. 2015. Both the concentration and redox state of glutathione and ascorbate influence the sensitivity of Arabidopsis to cadmium. *Annals of Botany* **116**: 601–612.

Jozefczak M, Keunen E, Schat H, Bliek M, Hern Andez LE, Carleer R, Remans T, Bohler S, Vangronsveld J, Cuypers A. 2014. Differential response of Arabidopsis leaves and roots to cadmium: glutathione-related chelating capacity vs antioxidant capacity. *Plant Physiology and Biochemistry* **83**: 1–9.

Krämer U. 2010. Metal hyperaccumulation in plants. *Annual Review of Plant Biology* **61**: 517–534.

Krebs M, Beyhl D, Görlich E, Al-Rasheid KAS, Marten I, Stierhof Y-D, Hedrich R, Schumacher K. 2010. Arabidopsis V-ATPase activity at the tonoplast is required for efficient nutrient storage but not for sodium accumulation. *Proceedings of the National Academy of Sciences, USA* **107**: 3251–3256.

Li H, Yu M, Du X-Q, Wang Z-F, Wu W-H, Quintero FJ, Jin X-H, Li H-D, Wang Y. 2017. NRT1.5/NPF7.3 functions as a proton-coupled H^+/K^+ antiporter for K^+ loading into the xylem in Arabidopsis. *Plant Cell* **29**: 2016–2026.

Li S, Yu J, Zhu M, Zhao F, Luan S. 2012. Cadmium impairs ion homeostasis by altering K^+ and Ca^{2+} channel activities in rice root hair cells. *Plant, Cell & Environment* **35**: 1998–2013.

Love MI, Huber W, Anders S. 2014. Moderated estimation of fold change and dispersion for RNA-seq data with DESeq2. *Genome Biology* **15**: 550.

Maere S, Heymans K, Kuiper M. 2005. BiNGO: a cytoscape plugin to assess overrepresentation of gene ontology categories in biological networks. *Bioinformatics* **21**: 3448–3449.

Martos S, Gallego B, Sáez L, López-Alvarado J, Cabot C, Poschenrieder C. 2016. Characterization of zinc and cadmium hyperaccumulation in three *Noccaea* (Brassicaceae) populations from non-metalliferous sites in the Eastern Pyrenees. *Frontiers in Plant Science* **7**: 128.

Mei H, Cheng NH, Zhao J, Park S, Escareno RA, Pittman JK, Hirschi KD. 2009. Root development under metal stress in *Arabidopsis thaliana* requires the H^+/cation antiporter CAX4. *New Phytologist* **183**: 95–105.

Mendoza-Cózatl DG, Xie Q, Akmakjian GZ, Jobe TO, Patel A, Stacey MG, Song L, Demoin DW, Jurisson SS, Stacey G *et al.* 2014. OPT3 is a component of the iron-signaling network between leaves and roots and misregulation of *OPT3* leads to an over-accumulation of cadmium in seeds. *Molecular Plant* **7**: 1455–1469.

Menzies NW, Donn MJ, Kopittke PM. 2007. Evaluation of extractants for estimation of the phytoavailable trace metals in soils. *Environmental Pollution* **145**: 121–130.

Meyer C-L, Juraniec M, Huguet S, Chaves-Rodriguez E, Salis P, Isaure M-P, Goormaghtigh E, Verbruggen N. 2015. Intraspecific variability of cadmium tolerance and accumulation, and cadmium-induced cell wall modifications in the metal hyperaccumulator *Arabidopsis halleri*. *Journal of Experimental Botany* **66**: 3215–3227.

Morel M, Crouzet J, Gravot A, Auroy P, Leonhardt N, Vavasseur A, Richaud P. 2009. AtHMA3, a P1B-ATPase allowing Cd/Zn/Co/Pb vacuolar storage in Arabidopsis. *Plant Physiology* **149**: 894–904.

Morreel K, Saeys Y, Dima O, Lu F, Van De Peer Y, Vanholme R, Ralph J, Vanholme B, Boerjan W. 2014. Systematic structural characterization of metabolites in *Arabidopsis* via candidate substrate-product pair networks. *Plant Cell* **26**: 929–945.

Nakabayashi R, Yonekura-Sakakibara K, Urano K, Suzuki M, Yamada Y, Nishizawa T, Matsuda F, Kojima M, Sakakibara H, Shinozaki K *et al.* 2014. Enhancement of oxidative and drought tolerance in Arabidopsis by overaccumulation of antioxidant flavonoids. *Plant Journal* **77**: 367–379.

Novikova PY, Hohmann N, Nizhynska V, Tsuchimatsu T, Ali J, Muir G, Guggisberg A, Paape T, Schmid K, Fedorenko OM *et al.* 2016. Sequencing of the genus *Arabidopsis* identifies a complex history of nonbifurcating speciation and abundant trans-specific polymorphism. *Nature Genetics* **48**: 1077–1082.

Okamoto M, Kumar A, Li W, Wang Y, Siddiqi MY, Crawford NM, Glass ADM. 2006. High-affinity nitrate transport in roots of Arabidopsis depends on expression of the *NAR2*-like gene *AtNRT3.1*. *Plant Physiology* **140**: 1036–1046.

Pauwels M, Vekemans X, Godé C, Frérot H, Castric V, Saumitou-Laprade P. 2012. Nuclear and chloroplast DNA phylogeography reveals vicariance among European populations of the model species for the study of metal tolerance, *Arabidopsis halleri* (Brassicaceae). *New Phytologist* **193**: 916–928.

Pineau C, Loubet S, Lefoulon C, Chalies C, Fizames C, Lacombe B, Ferrand M, Loudet O, Berthomieu P, Richard O. 2012. Natural variation at the *FRD3* MATE transporter locus reveals cross-talk between Fe homeostasis and Zn tolerance in *Arabidopsis thaliana*. *PLoS Genetics* **8**: e1003120.

Plaza S, Tearall KL, Zhao FJ, Buchner P, McGrath SP, Hawkesford MJ. 2007. Expression and functional analysis of metal transporter genes in two contrasting ecotypes of the hyperaccumulator *Thlaspi caerulescens*. *Journal of Experimental Botany* **58**: 1717–1728.

Pound MP, French AP, Atkinson JA, Wells DM, Bennett MJ, Pridmore T. 2013. RootNav: navigating images of complex root architectures. *Plant Physiology* **162**: 1802–1814.

Pueyo M, López-Sánchez J, Rauret G. 2004. Assessment of $CaCl_2$, $NaNO_3$ and NH_4NO_3 extraction procedures for the study of Cd, Cu, Pb and Zn extractability in contaminated soils. *Analytica Chimica Acta* **504**: 217–226.

Qi T, Song S, Ren Q, Wu D, Huang H, Chen Y, Fan M, Peng W, Ren C, Xie D. 2011. The jasmonate-ZIM-domain proteins interact with the WD-Repeat/bHLH/MYB complexes to regulate jasmonate-mediated anthocyanin accumulation and trichome initiation in *Arabidopsis thaliana*. *Plant Cell* **23**: 1795–1814.

Ravichandran R, Rajendran M, Devapiriam D. 2014. Antioxidant study of quercetin and their metal complex and determination of stability constant by spectrophotometry method. *Food Chemistry* **146**: 472–478.

Rouquié D, Tournaire-Roux C, Szponarski W, Rossignol M, Doumas P. 1998. Cloning of the V-ATPase subunit G in plant: functional expression and subcellular localization. *FEBS Letters* **437**: 287–292.

Sambade M, Alba M, Smardon AM, West RW, Kane PM. 2005. A genomic screen for yeast vacuolar membrane ATPase mutants. *Genetics* **170**: 1539–1551.

Sarret G, Saumitou-Laprade P, Bert V, Proux O, Hazemann J-L, Traverse A, Marcus MA, Manceau A. 2002. Forms of zinc accumulated in the hyperaccumulator *Arabidopsis halleri*. *Plant Physiology* **130**: 1815–1826.

Schindelin J, Arganda-Carreras I, Frise E, Kaynig V, Longair M, Pietzsch T, Preibisch S, Rueden C, Saalfeld S, Schmid B *et al.* 2012. Fiji: an open-source platform for biological-image analysis. *Nature Methods* **9**: 676–682.

Schvartzman MS, Corso M, Fataftah N, Scheepers M, Nouet C, Bosman B, Carnol M, Motte P, Verbruggen N, Hanikenne M. 2017. Adaptation to high zinc depends on distinct mechanisms in metallicolous populations of *Arabidopsis halleri*. *New Phytologist*. doi: 10.1111/nph.14949.

Siemianowski O, Barabasz A, Kendziorek M, Ruszczynska A, Bulska E, Williams LE, Antosiewicz DM. 2014. *HMA4* expression in tobacco reduces Cd accumulation due to the induction of the apoplastic barrier. *Journal of Experimental Botany* **65**: 1125–1139.

Stein RJ, Höreth S, de Melo JRF, Syllwasschy L, Lee G, Garbin ML, Clemens S, Krämer U. 2016. Relationships between soil and leaf mineral composition are element-specific, environment-dependent and geographically structured in the emerging model *Arabidopsis halleri*. *New Phytologist* **213**: 1274–1286.

Sze H, Schumacher K, Müller ML, Padmanaban S, Taiz L. 2002. A simple nomenclature for a complex proton pump: VHA genes encode the vacuolar H^+-ATPase. *Trends in Plant Science* **7**: 157–161.

Talke IN, Hanikenne M, Krämer U. 2006. Zinc-dependent global transcriptional control, transcriptional deregulation, and higher gene copy number for genes in metal homeostasis of the hyperaccumulator *Arabidopsis halleri*. *Plant Physiology* **142**: 148–167.

Ueno D, Milner MJ, Yamaji N, Yokosho K, Koyama E, Clemencia Zambrano M, Kaskie M, Ebbs S, Kochian LV, Ma JF. 2011. Elevated expression of *TcHMA3* plays a key role in the extreme Cd tolerance in a Cd-hyperaccumulating ecotype of *Thlaspi caerulescens*. *Plant Journal* **66**: 852–862.

Urquhart W, Chin K, Ung H, Moeder W, Yoshioka K. 2011. The cyclic nucleotide-gated channels AtCNGC11 and 12 are involved in multiple Ca^{2+}-dependent physiological responses and act in a synergistic manner. *Journal of Experimental Botany* **62**: 3671–3682.

Verbruggen N, Hermans C, Schat H. 2009. Molecular mechanisms of metal hyperaccumulation in plants. *New Phytologist* **181**: 759–776.

Verbruggen N, Juraniec M, Baliardini C, Meyer C-L. 2013. Tolerance to cadmium in plants: the special case of hyperaccumulators. *BioMetals* **26**: 633–638.

Verret F, Gravot A, Auroy P, Leonhardt N, David P, Nussaume L, Vavasseur A, Richaud P. 2004. Overexpression of AtHMA4 enhances root-to-shoot translocation of zinc and cadmium and plant metal tolerance. *FEBS Letters* **576**: 306–312.

Vert G, Grotz N, Dédaldéchamp F, Gaymard F, Guerinot ML, Briat J-F, Curie C. 2002. IRT1, an Arabidopsis transporter essential for iron uptake from the soil and for plant growth. *Plant Cell* **14**: 1223–1233.

Warren CR. 2008. Rapid measurement of chlorophylls with a microplate reader. *Journal of Plant Nutrition* **31**: 1321–1332.

Waters BM, Chu H-H, Didonato RJ, Roberts LA, Eisley RB, Lahner B, Salt DE, Walker EL. 2006. Mutations in Arabidopsis *Yellow Stripe-Like1* and *Yellow Stripe-Like3* reveal their roles in metal ion homeostasis and loading of metal ions in seeds. *Plant Physiology* **141**: 1446–1458.

Weber M, Harada E, Vess C, Roepenack-Lahaye EV, Clemens S. 2004. Comparative microarray analysis of *Arabidopsis thaliana* and *Arabidopsis halleri* roots identifies nicotianamine synthase, a ZIP transporter and other genes as potential metal hyperaccumulation factors. *Plant Journal* **37**: 269–281.

Weber M, Trampczynska A, Clemens S. 2006. Comparative transcriptome analysis of toxic metal responses in *Arabidopsis thaliana* and the Cd^{2+}-hypertolerant facultative metallophyte *Arabidopsis halleri*. *Plant, Cell & Environment* **29**: 950–963.

Willems G, Frérot H, Gennen J, Salis P, Saumitou-Laprade P, Verbruggen N. 2010. Quantitative trait loci analysis of mineral element concentrations in an *Arabidopsis halleri* × *Arabidopsis lyrata petraea* F_2 progeny grown on cadmium-contaminated soil. *New Phytologist* **187**: 368–379.

Zhai Z, Gayomba SR, Jung H-I, Vimalakumari NK, Piñeros M, Craft E, Rutzke MA, Danku J, Lahner B, Punshon T *et al.* 2014. OPT3 is a phloem-specific iron transporter that is essential for systemic iron signaling and redistribution of iron and cadmium in *Arabidopsis*. *Plant Cell* **26**: 2249–2264.

Supporting Information

Additional Supporting Information may be found online in the Supporting Information tab for this article:

Fig. S1 Geographical origin and mineral element quantification of *Arabidopsis halleri* plants grown in their native site.

Fig. S2 Experimental design of hydroponic culture with PL22 and I16 *Arabidopsis halleri* populations.

Fig. S3 Validation of RNA-Seq results by qRT-PCR analysis.

Table S1 Primers used for qRT-PCR analysis

Table S2 RNA-Seq data and pairwise analysis results

Table S3 GO enrichment analysis on DEGs

Table S4 RNA-Seq counts and statistical analysis results for transporter, secondary metabolism and cell wall-related genes

Table S5 Metabolomic analysis on PL22 and I16 shoots

Methods S1 Physicochemical analysis and metal quantification in field samples, cDNA synthesis and qRT-PCR analysis, and ascorbic acid measurement by HPLC.

Please note: Wiley Blackwell are not responsible for the content or functionality of any Supporting Information supplied by the authors. Any queries (other than missing material) should be directed to the *New Phytologist* Central Office.